

Site and nature of H bonding on Ti (0001)

Peter J. Feibelman

Sandia National Laboratories, Albuquerque, New Mexico 87185*

D. R. Hamann

Bell Laboratories, Murray Hill, New Jersey 07974

F. J. Himpsel

IBM Watson Research Center, Yorktown Heights, New York 10598

(Received 4 April 1980)

The site and nature of the bonding of H at a Ti (0001) surface are established via the analysis of new angle-resolved photoemission measurements by self-consistent electronic-structure calculations. Experimentally observed H-induced surface states are identified with calculated bonding and antibonding combinations of H 1s and Ti 3d,4s orbitals. The positions of these levels are strongly dependent on local bonding geometry. The H site which minimizes the total energy gives a very good account of the observed spectrum. Ignoring the total energy leads to a more ambiguous structure determination.

The fundamental problems of current surface science are the determination of surface atomic arrangement and of the forces that lead to it. Of various approaches to solving these problems, the analysis of valence spectroscopic data is important because at the same time as one fits theory to measurement, one explores the electronic rearrangements that are responsible for surface geometry. Previous efforts in this direction, for Pd (111)-H (1×1) (Ref. 1) and Ti (0001)-H (1×1) (Ref. 2), have been promising in showing that even angle-integrated electron-spectroscopic predictions are sensitive to bonding geometry. However, polarization-dependent angle-resolved ultraviolet-photoemission-spectroscopy (PARUPS) data provide a great deal more information (level symmetries, orderings, and dispersions) than is available in ordinary angle-integrated ultraviolet-photoemission spectroscopy (UPS). A complete set of PARUPS measurements thus presents a much more stringent test of a hypothetical geometry and corresponding electronic-structure analysis.

Nevertheless in the present work, for H on single crystal Ti (0001), we find that even an extensive set of PARUPS results is not enough to determine the bonding geometry unambiguously. Comparison of spectroscopic predictions to PARUPS surface-band positions and dispersions *does* make it possible to eliminate many bonding geometries and stoichiometries. But, given the poor current knowledge of the degree to which a local-exchange-correlation model band structure *should* agree with a measured excitation spectrum, we find several H-bonding sites which are spectroscopically "acceptable." Only when we consider the total energy can we eliminate the remaining ambiguity in the surface-structure determination.

By analyzing the PARUPS results we find that H on Ti (0001) adsorbs as a 1×1 overlayer via the formation of a H 1s-Ti 3d bonding surface band over the entire surface Brillouin zone (SBZ). In the central portion of the SBZ *two* H-induced surface features are observed at each \vec{k}_{\parallel} (1.3 and 6.9 eV below E_F , respectively, at Γ). The upper surface state is unusual and particularly interesting in that its energy is in the region of the Ti d bands, far above the H 1s level. We find that these zone-center surface features correspond to combinations of H 1s and Ti $3d_{3z^2-r^2}$, 4s orbitals. Their energy locations depend strongly on the local H-Ti geometry: As the overlap of the H 1s and Ti $3d_{3z^2-r^2}$ wave functions increases, the splitting of the bonding-antibonding pair increases, ultimately driving the antibonding state out of a large bulk band gap up into a bulk band wherein it disappears as an observable surface feature. The sensitivity of these spectral features to bonding geometry makes it easy to tell in advance which geometries will yield reasonable spectroscopic predictions and several do. Satisfyingly, the minimum total-energy configuration is one of those which is spectroscopically acceptable.

Our calculations predict the observed work function difference of about 0.2 eV between the clean and H-covered Ti (0001) films, although the calculated *absolute* work functions are about 0.8 eV smaller than measured. The theoretical core-level energies for surface Ti's show an appreciable dependence on the H location.

The Ti-H bond length (3.6 a.u.) which minimizes the total energy is roughly that of TiH₂, corresponding to an H radius of ~0.9 a.u., about 50% larger than the H radius found by Louie to describe UPS data for H coordinated similarly on Pd (111).¹ We

attribute this difference to the partial occupation of the antibonding H-induced state in Ti as against the nonoccupation of the antibonding H-Pd states in the latter system.

The H-Ti system is a particularly interesting one for study. Ti reacts readily with H making it the single most important getter material for H. Ti forms a bulk hydride and the reaction of H with Ti surfaces determines the uptake of H in hydrogen storage applications.³

Since H reacts so readily with Ti, extensive heat cycling (up to $\sim 800^\circ\text{C}$) was necessary during sputter cleaning to deplete bulk and surface of hydrogen. Exposure to H_2 resulted in a saturation of the intensity of hydrogen-induced features at 2 L [1 L (langmuir) = 10^{-6} Torr s]. This surface gave a clear 1×1 low-energy electron diffraction (LEED) pattern. The 1×1 structure is confirmed by our photoemission results. In particular, the higher-lying H-induced surface state is only found near the center of the 1×1 surface Brillouin (SBZ). This excludes surface umklapp effects.⁴

Angle-integrated photoelectron spectra for clean, H-covered (and also N-covered) Ti (0001) have been presented in an earlier publication (see Fig. 5 of Ref. 5). The clean surface shows a strong feature near E_F which is identified with a predicted² band of surface states. These states are quenched by H adsorption, suggesting an overlayer geometry,^{2,6} in contrast to the situation for an N (1×1) "underlayer,"⁷ which does not quench the E_F surface-state band.⁵ Structures in the angle-integrated data for clean Ti (0001) are found at -0.8 and -2.1 eV. They are characteristic of the bulk Ti density of states (DOS), and accordingly they remain for Ti (0001)-H (1×1). H-induced features in the angle-integrated results are observed from -4.5 to -7 eV and at -1.3 eV.

Examining the H-induced features as a function of electron exit angle and photon polarization, we find quite dramatic effects, indicating at the outset that the H adlayer is very well ordered. As an example, in Fig. 1(b) we show normal emission spectra for two polarizations, both at $h\nu = 22$ eV. The H-induced state at -1.3 eV is barely seen in s polarization, while it is very intense (much more so than in the angle-integrated data) when the light has a p-polarized component. Using dipole selection rules⁸ we thus determine the symmetry of this state to be Λ_1 . As $h\nu$ is varied at normal emission, the -1.3 -eV state does not disperse, as a surface state should not, while the cross section exhibits a strong resonance at $h\nu \sim 25$ eV. One also sees in the lower panel of Fig. 1 the bonding surface state as an enhancement near -6.9 eV. The other features in that panel correspond to bulk Ti states.⁹

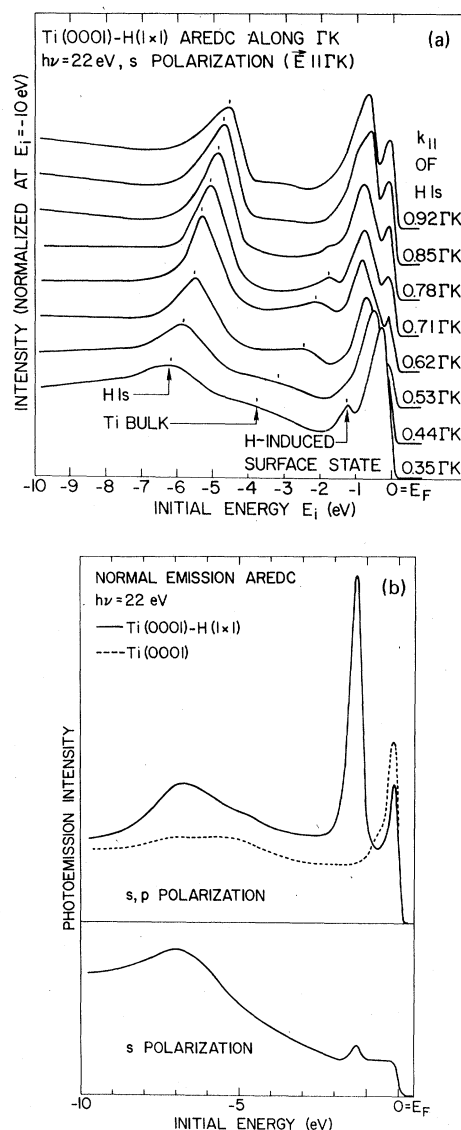


FIG. 1. (a) E vs $\vec{k}_{||}$ dispersion for the bonding H's band along KM ($\Gamma-K = 1.42 \text{ \AA}^{-1}$). The electric vector lies in the escape plane. (b) Normal emission photoelectron spectra for Ti (0001) and Ti (0001)-H (1×1) for mixed s, p polarization and pure s polarization. This panel shows the location of the H-induced state at -1.3 eV and its Λ_1 symmetry.

Off-normal emission data are shown in Fig. 1(a), selecting the detection geometry such that $\vec{k}_{||}$ lies along the $\Gamma-K$ line in the SBZ. For small $\vec{k}_{||}$ a remnant of the H-induced state is still seen at -1.3 eV. The prominent feature which disperses from -6.15 eV at $0.35 \Gamma-K$ to -4.55 eV at $0.92 \Gamma-K$ is the H-induced bonding band. Its dispersion is independent of $h\nu$ as one would expect. The other structures in the data can be explained at Ti bulk interband transitions via their dispersion

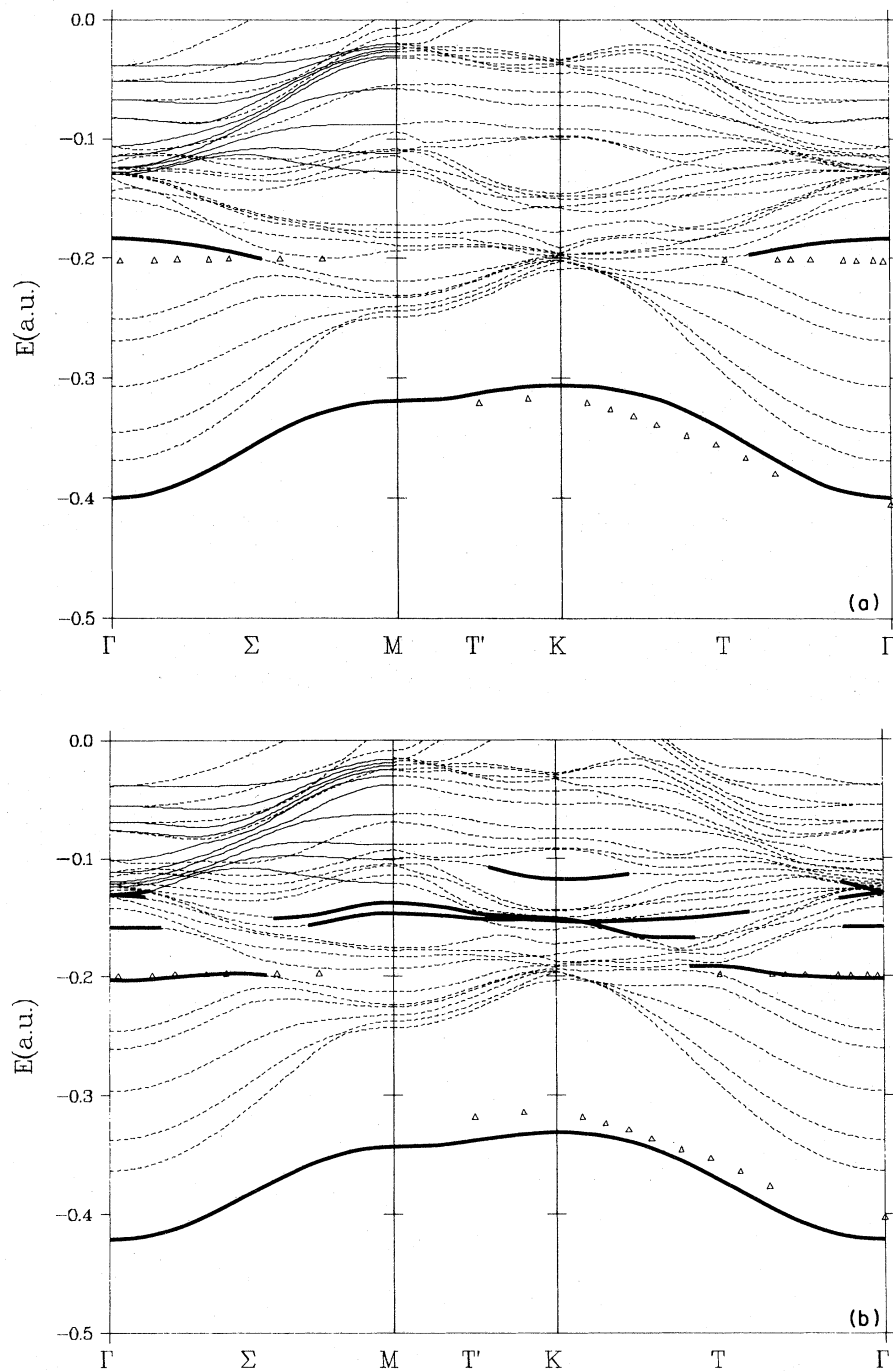


FIG. 2. Comparison of calculated and measured (relative to E_F) energy-band dispersions for two bonding sites of H in Ti (0001)-H (1×1). The data are represented by triangles. The heavy lines are states with high wave-function amplitude in the surface layers. Along M the dashed and solid lines are even and odd states with respect to reflection in the (0001) surface mirror plane. The calculations are for an 11-layer Ti film with an adlayer of H on both sides. Only states even under reflection in the central plane are shown. (a) The H sits in an fcc overlayer site with the Ti-H bond length that of TiH_2 and no relaxation of the outer Ti layers' separation. This is the lowest total-energy site of the ~ 25 that we have studied. $E_F = -0.153$ a.u. in this case. (b) The H sits in a tetrahedral underlayer site directly above a Ti atom. The outer Ti-layer separation is 30% greater than in bulk Ti and the Ti-H bond length is that of TiH_2 . $E_F = -0.150$ a.u. in this geometry.

with $h\nu$ at fixed \vec{k}_{\parallel} (not shown here).

Figure 2 compares theoretical and experimental energy-band dispersions along the perimeter of the irreducible $\frac{1}{12}$ of the SBZ, for two different H adsorption geometries (of ~ 25 that we have studied). In both cases we have one H per surface Ti (Ref. 10), and a Ti-H bond length equal to that of TiH_2 . In Fig. 2(a) the H atoms are symmetrically located in a threefold coordination site with no second-layer Ti atom directly below (an "fcc" site), and no relaxation of the separation between the outer two Ti layers. Figure 2(b) corresponds to having the H's below the first Ti layer directly above a second-layer Ti atom, with the outer two Ti layers' separation equal to 1.3 times the bulk interlayer spacing. (This is an asymmetric "tetrahedral" geometry.) The experimental positions of the H-induced surface states are indicated by triangles.

Our purpose in comparing Figs. 2(a) and 2(b) is to show a potential difficulty in relying purely on a comparison of calculated and measured spectra to determine an adsorption geometry. Specifically, one notes that for these very different geometries the H-induced levels' dispersions are fitted equally well. In the fcc geometry the upper surface state is ~ 0.5 eV too high, while in the tetrahedral case the deep state is ~ 0.5 eV too low. The fcc geometry is favored spectroscopically if one considers the spectrum near E_F , in that it leads to a quenching of the E_F surface band, as is generally true for overlayers,^{2,6} while the tetrahedral site does not, as is generally found for underlayers.^{2,5,6} On the other hand, one might argue that since the E_F surface band is quite narrow, physical or calculational inaccuracies that moved it down by a few tenths of an eV would make it appear that this band is occupied when in reality it is not. This argument is rather weak, considering that the occupied portions of the E_F surface bands for this geometry contain ~ 2 electrons and are thus electrostatically stabilized. But, in any case, the issue can be settled convincingly by calculating the heat of adsorption in the proposed sites.

Total-energy calculations have been incorporated with the previously described self-consistent linear combination of atomic orbitals (LCAO) method.¹¹ The valence kinetic energy is calculated directly from the wave functions. The valence-valence and valence- (rigid) core electrostatic energies are calculated using the charge as fitted by the auxiliary charge-potential basis functions.¹¹ This step, which is a practical computational necessity for an extended system, prevents the total energy from being a strict variational quantity. The local exchange-correlation (xc) energy is

calculated by first finding the difference between the xc energy density of the total fitted charge and that of the core charge alone in real space. This energy density difference is then least-squares fitted and integrated analytically. These procedures avoid the problem of numerically subtracting energies containing large core contributions.

The H heat of adsorption is calculated by subtracting the valence total energies of the Ti-H film from that of a clean Ti film plus atomic H. Most systematic errors due to the auxiliary fitting function basis can be assumed to cancel in the difference. Tests performed by varying this basis indicated that residual uncertainties are in the 0.1-eV range.

We find that the heat of adsorption per H atom is ~ 1.1 eV greater in the fcc overlayer site than in the asymmetric tetrahedral geometry. The accuracy of the basic physical approximation, local exchange, and correlation, for the heat of adsorption in the Ti-H system is directly verified in that we find that the heat of adsorption of H in the most favorable underlayer geometry, with H in a symmetric octahedral ("oct") site, to be 2.6 eV, while the measured heat of solution of H in Ti (Ref. 12) is 2.7 eV. Incidentally, we calculate that overlayer sites are *generally* more tightly bound than underlayer sites (see Table I), by ~ 0.5 to ~ 1 eV, because of the weakening of Ti-Ti bonds as the more electronegative H's remove electrons from them. Overlayer H is bound by Ti electrons that are engaged in Ti-Ti bonding to a much smaller extent. This result agrees with the finding that H dissolves into Ti as the temperature is raised and returns to the surface when it is lowered.

In summary, once one has established the regularities according to which the predicted spectroscopy varies with the assumed surface geometry (cf. below), it may be possible to find several geometries which give an acceptable fit to angle-resolved ultraviolet-photoemission-spectroscopy (ARUPS) measurements. In this circumstance an evaluation of the total energy of the system versus adsorption geometry is invaluable in deciding which geometry is the most likely to be correct. This fact is illustrated in Table I, which shows that the fcc geometry corresponding to Fig. 2(a) has the lowest total energy of several geometries whose spectra are reasonably good in comparison to measurements.

Another *caveat* concerning the determination of surface geometry by fitting surface-band positions concerns correlation effects. As is seen in Figs. 2, the upper H-induced surface band is extremely flat. Thus the band corresponds to very localized states and one should not *expect* a local exchange-correlation calculation to fit its position accurately.

TABLE I. Comparison of calculated electronic structure results for three underlayer (oct and tet) and four overlayer (hcp and fcc) geometries, with ARUPS data. In the table, bond length=sym means H at the symmetry site, $r=0.6$ a.u. means the H radius is 0.6 a.u., and TiH_2 means that the Ti-H distance is that of TiH_2 . Expansion refers to the percent expansion of the outer Ti-layers' separation. HA(H) is the calculated H heat of adsorption. $\delta\Phi$ is the H-induced work function shift, $AB(\Gamma)$, $B(\Gamma)$, $B(K)$ are the H-induced antibonding- and bonding-level positions relative to the Fermi energy (the calculated E_F for the theoretical cases and the experimental E_F for the UPS data) at the points Γ and K in the SBZ. Notice that although the H-induced levels agree rather well with experiment for several geometries, the fcc, TiH_2 , 0% case is favored by 0.2 eV/H in E_{tot} over any other case. Also (compare Fig. 3) note the systematic variation of bonding- and antibonding-level positions with bond angle. E_{core} is the difference between surface and interior Ti core-level binding energies.

Site	Oct	Tet	Tet	fcc	hcp	fcc	fcc	Expt.
Bond length	sym	sym	TiH_2	$r=0.6$ a.u.	TiH_2	TiH_2	TiH_2	?
Expansion	0%	0%	30%	0%	0%	0%	20%	?
HA(H)	2.6 eV	2.3 eV	2.3 eV	3.0 eV	3.1 eV	3.3 eV	2.9 eV	?
$\delta\Phi$	0.1 eV	0.4 eV	0.2 eV	-0.4 eV	0.5 eV	0.3 eV	0.2 eV	0.2-0.3 eV
$AB(\Gamma)$	0.7 eV	0.4 eV	1.4 eV		0.8 eV	0.8 eV	1.1 eV	1.3 eV
$B(\Gamma)$	8.2 eV	8.2 eV	7.4 eV	7.2 eV	6.7 eV	6.7 eV	6.6 eV	6.9 eV
$B(K)$	6.1 eV	6.2 eV	4.9 eV	4.8 eV	4.1 eV	4.2 eV	4.2 eV	4.5 eV
E_{core}	-0.20 eV	-0.33 eV	-0.28 eV	0 eV	-0.25 eV	-0.25 eV	-0.22 eV	?

ly. This is another reason why the total energy is an important guide to which of several acceptable geometries is best.

We now wish to discuss the nature of the H-induced surface states and how their positions are influenced by adsorption geometry. The deep H-induced band consists of bonding combinations of H 1s, Ti 3d, and Ti 4s orbitals. By symmetry the Ti contributions near Γ have 4s and $3d_{3z^2-r^2}$ characters and in the outer part of the SBZ they are largely $3d_{x^2-y^2,xy}$ and $3d_{xz,yz}$. Since there is evidently much more outer than central part of the SBZ, it is clear that the Ti-H bond is formed with the x^2-y^2,xy and xz,yz orbitals of the Ti. [The only geometry we tried that did not lead to a deep bonding band is the atop (onfold) coordination geometry.² In this case the H 1s has its strongest overlap with the $\text{Ti } 3d_{3z^2-r^2}$ orbital. Since this orbital character lies at low energies only near Γ , the "terminal" bond is weak, and one can conclude straightforwardly that onfold coordination is unlikely to occur.]

An examination of the orbital coefficients for the high-lying surface state, e.g., for the fcc geometry of Fig. 2(a), shows that it is an antibonding combination of H 1s orbitals largely with $\text{Ti } 3d_{3z^2-r^2}$ states. Thus near Γ the upper and lower H-induced surface states are an occupied pair of antibonding and bonding states. Accordingly one expects that any change in bonding geometry that increases the overlap of the H 1s and $\text{Ti } 3d_{3z^2-r^2}$ orbitals will push the bonding state down and the antibonding state up in energy. In the geometry which we earlier found to give the "best" description of Eastman's angle-integrated UPS data from evaporated polycrystalline Ti covered with H (Ref. 13)

there was no upper surface state near Γ .² This geometry corresponded to assuming a H radius $r(\text{H}) \sim 0.6$ a.u., which as is shown in Fig. 3, results in a considerably greater H 1s-Ti $3d_{3z^2-r^2}$ overlap than one has, assuming the same threefold overlayer coordination (hcp or fcc (Ref. 14)), but $r(\text{H}) \sim 0.9$ a.u. (corresponding to the TiH_2 bond length). Thus in the $r(\text{H}) \sim 0.6$ a.u. geometry, the bonding state is somewhat deeper than in the fcc TiH_2 bond-length geometry of Fig. 2(a), and the antibonding

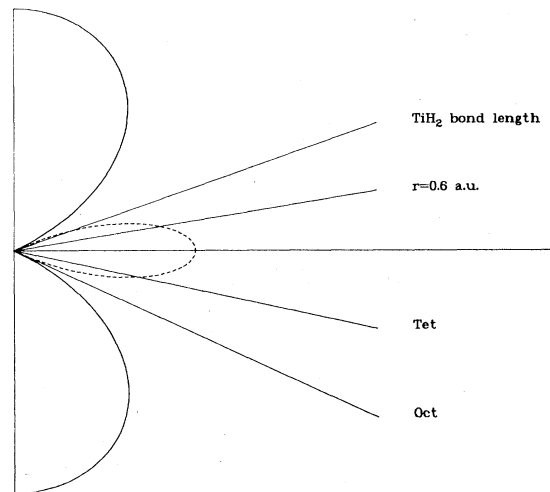


FIG. 3. Bond angles and relative lengths for various H-bonding sites shown relative to a $3z^2-r^2$ orbital. As the bond angle gets lower, the bond length becomes shorter, and the H 1s-Ti $3d_{3z^2-r^2}$ bonding and antibonding levels are driven down and up, respectively, by the increasing overlap. See Table I. (The Tet label here refers to H at the symmetry site with the outer Ti layers unexpanded.)

state does not exist because it has been pushed up into the bulk bands.

The geometry of this simple picture is illustrated in Fig. 3 and the consequences are shown in Table I. In Fig. 3 it is shown that the H sites corresponding to larger bond angles with the surface have reduced overlap with the Ti $3d_{3z^2-r^2}$ orbital both because the bond angle is closer to the nodal plane of this orbital and because the bond length is longer. Table I then shows that this reduced overlap results in a deeper antibonding state and a higher bonding state.

This overlap argument provides a lowest-order rule for adjusting the spectroscopy by modifying the adsorption geometry. Next-order adjustments of the spectrum can be obtained by varying the spacing of the first two Ti layers although here the physics is still obscure.

In view of the excellent agreement we have found between total energy calculations, predicted spectroscopy, and ARUPS data referred to the Fermi energy, it is puzzling that the predicted and measured absolute work functions Φ for clean and H covered Ti (0001) differ in both cases by about 0.8 eV although we know that Φ is considerably more sensitive than these other calculated results to the choice of charge-fitting basis. It is possible that a low level of surface impurities, e.g., O, could have increased the measured work functions to this degree. On the other hand, the Gaussian basis functions used to describe the clean and H-covered surfaces are sufficiently different that it

is hard to see why they both should have led to the same work-function discrepancy. Calculations based on a different approximation scheme may help settle this issue.

In conclusion we would like to call attention to the geometry dependence of the surface-bulk core-level shifts we have found (see Table I). Generally, the core levels are shifted to greater binding energy in the surface Ti's by amounts varying from 0.0 to 0.5 eV, depending on adsorption geometry. The cases for which the shift is zero are those in which there is no important band of surface states near the Fermi level. This is a simple result—it says that when the surface Ti valence electrons occupy states similar to those of the bulk Ti's there is no core-level shift.

The simple physics underlying the variation of the Ti-H system's spectroscopy and the fact that our total energy calculation appears to be reliable, suggests that current electronic-structure methods are adequate to help us determine adsorption geometry and the nature of the chemisorption bond on metals. Accordingly we foresee a great deal more work in this area in the near term.

ACKNOWLEDGMENTS

The portion of this work performed at Sandia Laboratories was supported by the U. S. Department of Energy, DOE, under Contract No. DE-AC04-76-DP00789. We would like to thank J. W. Rabalais for providing the crystal used in this study.

*A U. S. Department of Energy facility.

¹S. G. Louie, Phys. Rev. Lett. **42**, 476 (1979).

²P. J. Feibelman and D. R. Hamann, Phys. Rev. B **21**, 1385 (1980).

³M. A. Pick, J. W. Davenport, M. Strongin, and C. J. Diener, Phys. Rev. Lett. **43**, 286 (1979).

⁴J. Anderson and G. J. Lapeyre, Phys. Rev. Lett. **36**, 376 (1976).

⁵P. J. Feibelman and F. J. Himpsel, Phys. Rev. B **21**, 1394 (1980).

⁶P. J. Feibelman and D. R. Hamann, Solid State Commun. **34**, 215 (1980).

⁷H. D. Shih, F. Jona, D. W. Jepsen, and P. M. Marcus, Surf. Sci. **60**, 445 (1976).

⁸F. J. Himpsel and D. E. Eastman, Phys. Rev. B **20**, 3217 (1979).

⁹The polarization-independent structure at -7.0 eV in the panel of Fig. 1 is due to a final-state structure 15 eV above E_F in the secondaries, which is unaffected by H. The structure at -5.0 eV is a bulk interband transition, whose dispersion with \vec{k}_{\parallel} can be seen in the panel.

¹⁰We have also studied the possibility of two H's per surface Ti. This situation causes the deep H-surface state to fold back into a rapidly dispersing H-H antibonding band. The dispersion of this band is *much* greater than that of the observed upper H-induced surface band and the bonding band is pushed much too low in comparison with UPS data for this stoichiometry to be plausible. Moreover, the bonding-antibonding pair of states would show up as a deep doublet in the outer part of the SBZ, which is not seen. This fact also rules out the 2 H-to-one surface-Ti stoichiometry.

¹¹Our method is described at length in P. J. Feibelman, J. A. Appelbaum, and D. R. Hamann, Phys. Rev. B **20**, 1433 (1979).

¹²W. M. Mueller, in *Metal Hydrides*, edited by W. M. Mueller, J. P. Blackledge, and G. G. Libowitz (Academic, New York, 1968), p. 367.

¹³D. E. Eastman, Solid State Commun. **10**, 933 (1972).

¹⁴The inequivalent threefold sites (hcp and fcc) were indistinguishable in a comparison with the angle-integrated UPS data of Ref. 16.